A Gaussian Filtering Method to Reduce Directionality on High-density Point Clouds Digitized by a Conoscopic Holography Sensor

Héctor Patiño [a], Pablo Zapico [a], J. Carlos Rico [a], Gonzalo Valiño [a,*], Pedro Fernández [a]

[a] *Department of Construction and Manufacturing Engineering, University of Oviedo, Campus de Gijón, 33203 Gijón, Spain*

[*] *Corresponding author. Tel.: +34 985182442. E-mail address: gvr@uniovi.es*

Abstract

This work analyses the directional effect shown by the high-density point clouds digitized with a conoscopic holography (CH) sensor. The asymmetric shape of the laser spot for this sensor yields directionality to appear along the largest spot dimension and to occur repeatedly under different working conditions. To study this effect, several digitizing tests were performed under different conditions on a surface machined by EDM with a uniform and isotropic finish, so that the directional effect should not appear. Nevertheless, the use of the 2D Fourier transform (2DFT) confirmed the existence of directionality in the point clouds along the largest spot direction and that it appeared repetitively under different working conditions. Thus, this effect could be considered as a systematic error associated to the CH sensor and then, feasible to be reduced. The use of an anisotropic 2D Gaussian filter is suggested for this purpose. The results found before and after applying the filter were compared to those obtained by a confocal microscope, which was used as reference due to its better metrological performance.

Keywords: Conoscopic holography, directionality, point clouds, Gaussian filter

1. Introduction

The industrial application of non-contact digitizing systems has grown importantly in recent years [1,2,3]. To a large extend, this is due to their ability to digitize small and complex geometric shapes, the high rate for points acquisition and their portability, which allows for installing them in different machines and production equipment.

Among the different digitizing systems, conoscopic holography (CH) is an interferometric collinear technique based on the double refractive property of birefringent crystals. It was first described by Sirat and Psaltis [4] and patented by Optimet Optical Metrology LTD. The underlying physical principle of measurement of this type of sensor is included in the guideline VDI/VDE 2617-6.2 [5].

The characteristics of point-type CH sensors include high accuracy and repeatability, good behaviour for a wide variety of materials, ability to digitize steep slope surfaces and feasibility to combine the sensor with different lenses to adapt it to various depths of field. As a collinear system, it can access to holes or narrow cavities by using simple devices for light redirection. All these characteristics make CH systems very useful in different fields of industry, such as quality assessment, reverse engineering or in-process inspection.

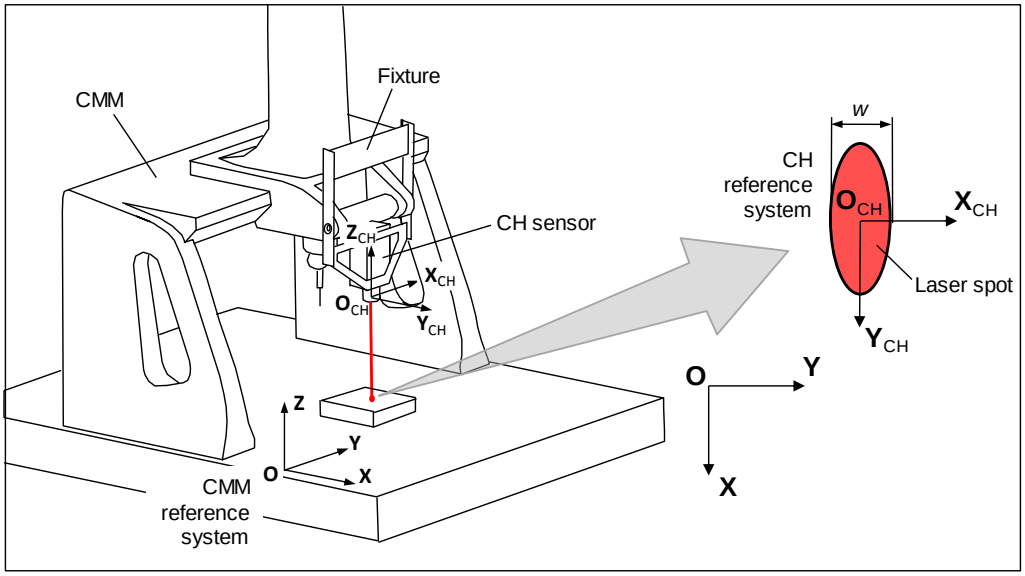

Fig. 1. Laser spot shape and orientation with respect to the CH and CMM coordinate systems

Nevertheless, CH digitizing quality may be affected by a lot of factors similarly to other optical techniques. Among these factors, one that affects to the quality of the digitized

surfaces is the *lateral resolution* of measurement or ability to recognize nearby points on a surface [6]. This concept is related to the minimum distance between these points and the size of the laser spot projected [7]. This way, as distance between points to be digitized is smaller and the size of the laser spot larger, higher overlapping between the spots appears.

The effect of *lateral resolution* could be resembled to a low pass filter that eliminates high frequencies of the digitized surface [8]. This is similar to the effect of digitizing a surface with a relatively large diameter contact probe, which is not able to access to the narrowest surface valleys, thus altering the measurement result.

Due to the asymmetry of the CH sensor laser spot used in this work (Fig. 1), the effect of *lateral resolution* is different depending on the digitizing direction. Thus, overlapping of laser spots will be higher when digitizing along the largest direction of the laser spot (Y_{CH}) than along the smallest one (X_{CH}). Consequently, when digitizing points separated from each other a distance shorter than the *lateral resolution*, this type of sensor will not allow for measuring high frequency details on the surface. Moreover, a directional behaviour can be perceived in the point cloud texture during the digitizing process (Fig. 2). In addition, the directional effect occurs along the largest spot direction and appears repeatedly under different working conditions, what reveals this effect as a sensor systematic factor feasible to be removed.

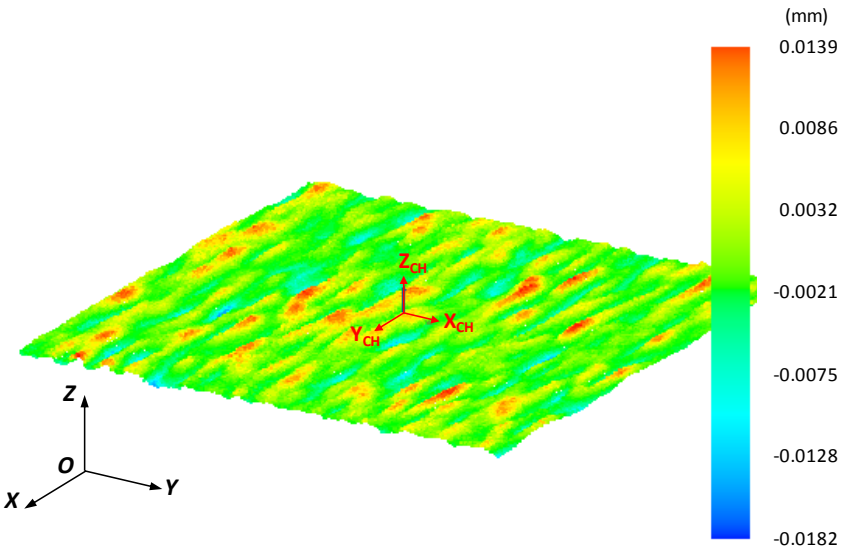

Fig. 2. Digitized 3D point cloud of a 2x2 mm flat surface machined by EDM

Directionality may be negligible when digitizing smooth and large sculptured surfaces, where high density of points is not required. However, when analyzing topographic features of a surface or when digitizing small-sized forms, this effect could mask the digitizing results. To eliminate this effect, the application of a Gaussian-type filter is proposed in this work. This type of filter is commonly used for the characterization of surfaces with high quality requirements, as it is described in [9,10]. In such cases, the filtering process extracts, from the surface topography, those components with frequencies related to roughness and removes those that become irrelevant [11−14].

In this work, a flat surface machined by EDM was used as test part in order to demonstrate that a directional effect appears in the point clouds digitized by a CH sensor. This effect was analyzed from both qualitative and quantitative points of view by using the 2D Fourier transform graphs of the point clouds and the complementary graphs of the *angular spectrum*. Both the directionality analysis and the Gaussian filter application were carried out under different process conditions and the results were compared with those obtained with a confocal microscope that were considered as reference.

2. Characteristics of the measuring system

The work described in this study was performed by means of the Conoscopic Holography (CH) sensor ConoPoint 10 by Optimet, equipped with two lenses of different focal length and different *depth of field* (DOF). The visible light source is a Class II laser diode which wavelength is 655 nm. This is a point-type sensor, thus each reading provides the value of the distance from the transmitter to the projection of the laser beam on the material surface (spot). In order to perform accurate sweeps of a surface, the CH sensor was integrated in a DEA Swift Coordinate Measuring Machine (CMM).

Table 1. Characteristics of the conoscopic holography sensor ConoPoint-10

Characteristic	**Lens 25 mm**	**Lens 50 mm**
Measuring frequency, F (Hz)	up to 9000	up to 9000
Power level, $P^{(1)}$ (%)	0 – 100	0 – 100
Depth of Field, DOF (mm)	1.8	8
Stand-off (mm)	14	44
Laser spot size (FWHM) $w^{(2)}$ (μm)	27	37

Repeatability [3] (μm)	0.06	0.10
Reproducibility 1σ [4] (μm)	0.4	1
Angular coverage (°)	150	170

[1] Maximum power level is equivalent to 1 mW

[2] Spot size is the effective width for measurement that contains 50% of the energy delivered, as measured at the centre of the working range.

[3] Standard deviation of 10 consecutive measurements performed on a diffusive metallic surface located in the middle of the DOF.

[4] As measured on a flat diffusive metallic surface, average of 5 scans offset in "y" direction. Minimum sampling step ½ of the spot size, average over 200 points in each scan. Measured over a step higher than 50% of the DOF.

4.1 Spot characteristics

The spot shape is elliptical and its minor and major axes are aligned with X_{CH} and Y_{CH} directions of the CH sensor, respectively (Fig. 1). Table 1 shows the main characteristics of the CH sensor for the lenses of 25 and 50 mm considered [15].

The sensor manufacturer considers that the light reflected by the different points illuminated by the laser spot varies according to a normal distribution. Thus, the central point of the spot will reflect the maximum power of light, decreasing as the points illuminated by the laser are far away from that position. Considering this type of distribution, the spot dimension w measured in the shortest spot direction, can be considered equivalent to the parameter FWHM (*Full Width at Half Maximum*) (Table 1). This value of w is provided for the spot at the *stand-off* distance but it increases as the spot is far from this position within the DOF. This parameter is commonly used to describe the width or the distance between points of a distribution curve when the corresponding function reaches half of its maximum value (Fig. 3). For a normal distribution, the value of the parameter FWHM is calculated as:

$$\mathrm{FWHM} = w = 2 \cdot \sqrt{2 \cdot ln2} \cdot s = 2.35482 \cdot s \quad (1)$$

where s represents the standard deviation of the normal distribution function.

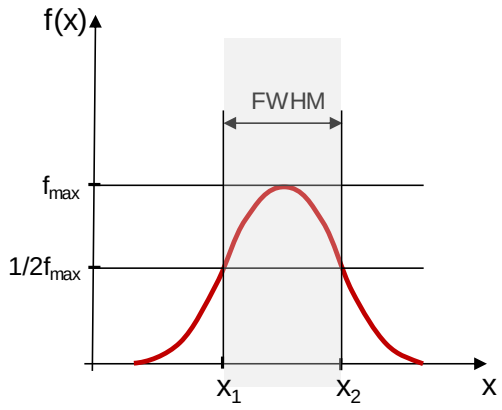

Fig. 3. Definition of *Full Width at Half Maximum* (FWHM)

4.1 Integration of the conoscopic holography sensor in a CMM

The CMM used in this work presents a maximum permissible error of length measurement ($E_{L,\,MPE}$) and a maximum permissible single stylus form error ($P_{FTU,\,MPE}$), which were certified according to ISO 10360-2 as follows:

$$E_{L,\,MPE} = 4\ \mu m + 4 \cdot 10^{-3} \cdot L, \text{ being L in mm} \tag{2}$$

$$P_{FTU,\,MPE} = 4\ \mu m \tag{3}$$

This CMM is operated by means of the measurement and control software PC-DMIS. The CH sensor was attached to the CMM carriage, so that it can be displaced along directions X (700 mm) and Y (450 mm) (Fig. 1). Although the sensor cannot be displaced along Z direction, the lens installed on the sensor allows for taking points located within the DOF. Therefore, all points captured may be represented by three coordinates. It is possible to adapt the measurement range in Z by using lenses with different DOF.

Once installed in the CMM, the CH sensor has to be calibrated to link the coordinates of any digitized point to the machine origin. The calibration procedure used in this work was inspired on the work by K. B. Smith [16].

In order to perform continues scanning instead of point-by-point scanning, X and Y movements of the CMM must be synchronized with the instant in which the CH sensor captures and registers the measurement of each point. For this, the CH sensor reads the pulses of the CMM encoders at a frequency of 25 MHz and uses them as triggering signals for taking the measurements. It was determined for the CMM used in this work that the distance traversed along an axis for each encoder rising edge is 0.004 mm. In

the tests, the distance between points captured was set to 0.004 mm in the Y direction, thus the triggering signal was activated for each rising edge.

4.1 Setting parameters of the conoscopic holography sensor

There are two main setting parameters in a CH sensor Conoprobe Point 10:

- *Power Level (P),* which represents the value of the laser beam energy and that can be set up in a range from 0 to 100% (maximum power level is equivalent to 1 mW).
- *Working Frequency (F),* which represents the data acquisition rate and that can be set up to a maximum of 9000 Hz.

For a given frequency, the value of power should be adjusted so that enough light power reaches the sensor. For a low level of power, the amount of light reflected off the surface that reaches the CCD could not be sufficient and then, quality of the measurement would drop. On the other hand, high values of power may yield a saturated signal so that measurements would not be reliable.

The initial adjustment of the CH sensor is carried out by tuning power and frequency until two indicators of signal quality are satisfied:

- *SNR* (Signal-to-Noise Ratio), which describes the quality of the signal for a digitized point. It is calculated by comparison of the signal power used for the measurement with the total reading, which includes signal noise. *SNR* may range from 0% to 100% and it is commonly assumed that the higher the *SNR*, the higher the accuracy of measurement. *SNR* should be above 50% to produce reliable measurement values.
- *Total*, which is the total amount of light detected by the CCD of the sensor in each measure. Acceptable values of Total should be between 1200 and 21000 [15].

3. Experimentation

In order to analyze the directionality of point clouds obtained with a CH sensor and the way to reduce this effect by means of a filtering process, several digitizing tests were carried out on a flat surface of 2x2 mm machined by EDM.

First, the specimen was digitized with a confocal microscope Leica DCM3D, which was used as reference due to the absence of directionality in the captured images. Table 2 shows the main characteristics of this microscope.

Table 2. Characteristics of the confocal microscope Leica DCM3D

Characteristic	Value
Objectives	From 2.5x to 150x
Vertical scanning range (mm)	40
Objectives magnification	5x
Numerical aperture	0.15
FOV (µm)	2550x1910
Optical resolution (X/Y) (µm)	0.94
Vertical resolution (nm)	<150

Next, digitizing was performed with the CH sensor in continuous mode and high density of points: 12 µm in the X axis and 4 µm in the Y axis of the CMM. Different lenses were used (25 and 50 mm) for digitizing the test part located at three positions within the DOF (10%, 50% y 90%) (Fig. 4)

Frequency of the CH sensor was set to 3000 Hz and power was adjusted according to the lens used in order to satisfy the recommended values of *SNR* and *Total*. Since no influence of the digitized surface location within the DOF was observed for the lens of 25 mm, power was adjusted to 17% of its maximum value. In the case of the lens of 50 mm, power was adjusted to 34% for the upper half of the DOF including the *stand-off*, and it was increased up to 39% for surfaces located within the lowest half of the DOF.

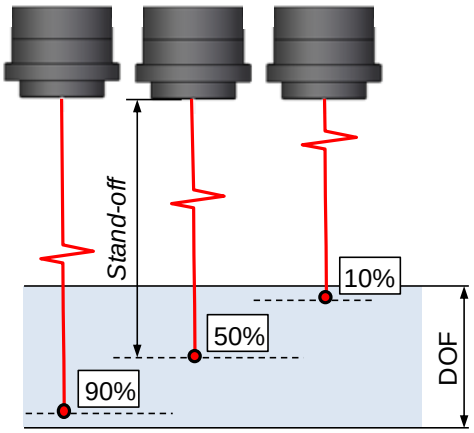

Fig. 4. Different locations of the digitized surface tested within the DOF

4. Directionality of the point clouds digitized by the CH sensor

When a surface is digitized by means of a CH sensor with an asymmetric laser spot, overlapping may occur between the spots corresponding to very close points, especially along the direction of the largest spot size (Y_{CH}).

Although the surfaces machined by EDM presented a very uniform topography and a high diffusion grade of the laser, during the digitizing of the specimen it was observed that the point cloud showed parallel fringes oriented along the largest spot direction (Y_{CH}) (Fig. 2). A 2D Fourier transform (2DFT) was used to check whether this directionality was significant or not. This function makes it possible to evaluate the different components of frequency observed on a surface in any direction of X-Y plane. In this work, 2DFT was applied to the Z value of the digitized points. From its representation, it can be interpreted whether it exists a directional effect.

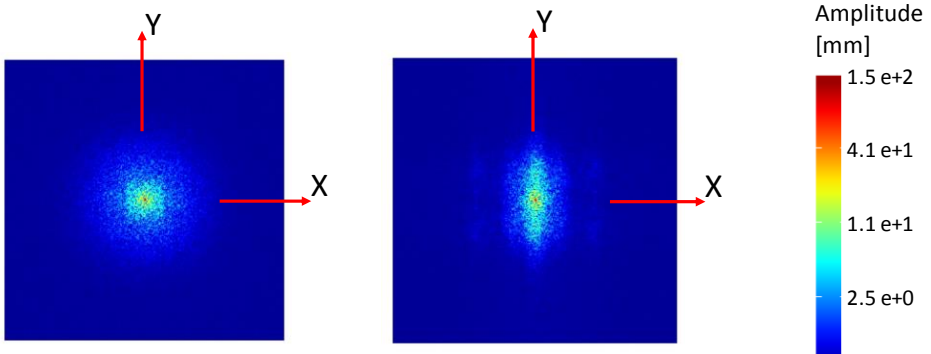

(a) Confocal microscope (b) Conoscopic holography

Fig. 5. 2DFT from the EDM surface digitized by the confocal microscope (a) and the CH sensor (b)

In order to analyze the obtained results, the surface machined by EDM was also digitized by means of a confocal microscope Leica DCM3D, which was used as reference due to its better metrological performance (Table 2). Thus, Fig. 5 shows the 2DFT graphs for a point cloud obtained by both the confocal microscope and the CH sensor.

For the 2DFT graph interpretation, it should be considered that X and Y axes represent frequencies and the origin of the graph represents the zero frequency point. All points at the same distance from the origin describe the amplitude of the surface spectrum for a certain frequency, while its angular position with respect to X and Y axes indicates the direction in which that amplitude occurs. Therefore, the wider the central area of the

graph, the larger the range of frequencies captured. At the same time, the farthest points from the origin represent the existence of high frequency noise, which are usually removed by means of filters, since they generally do not respond to the actual behavior of the surface but to the noise coupled to the measurement process.

Comparing the 2DFTs represented in Fig. 5, it can be seen that the symmetry of the spectrum is much greater in the case of the microscope, meaning that the digitized surface is very isotropic and has no directional effect. Isotropy responds to the finish uniformity expected on a surface obtained by EDM. In the case of the CH sensor, the lack of symmetry reveals a clear directionality that can be attributed exclusively to the sensor (Fig. 5b). Moreover, this effect was also observed along other digitizing directions using lenses with different focal length and even for different locations of the digitized surface within the lenses DOF. Thus, directionality is not dependent on external factors but it is intrinsically linked to the sensor, becoming a systematic effect.

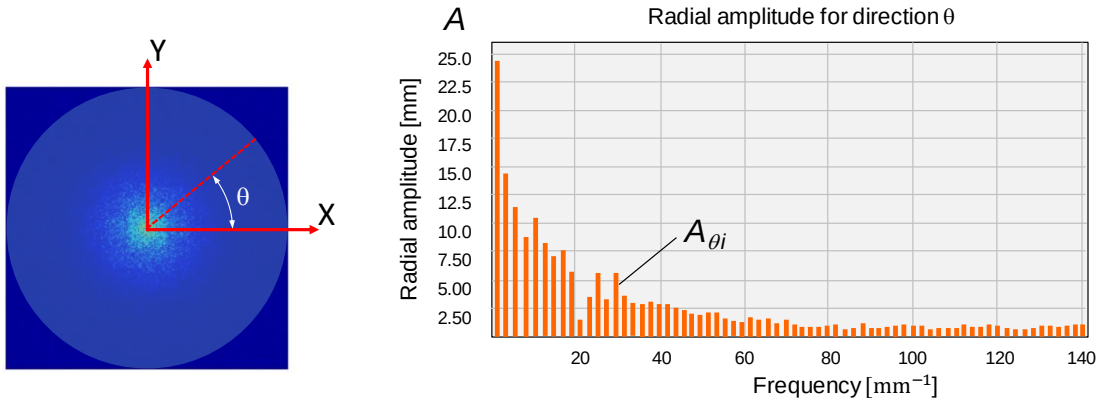

Fig. 6. Calculation example of accumulated radial amplitude for an angular direction θ of the 2DFT graph

4.1 Directionality measurement of the digitized surface

From the 2DFT, a complementary graph called *angular spectrum* [17] can be defined. For each angular direction θ, this graph represents the accumulated radial amplitude A_θ obtained as the sum of n amplitudes $A_{\theta i}$ corresponding to that direction (Fig. 6). That is:

$$A_\theta = \sum_1^n A_{\theta i} \quad \text{with } \theta = 0°, 1°, 2°, \dots, 360° \tag{4}$$

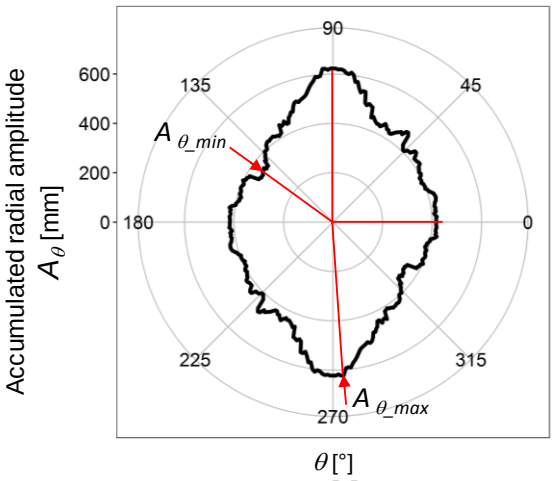

Fig. 7. Angular spectrum corresponding to a 2DFT graph

Fig. 7 represents an example of *angular spectrum* in which it can be seen if there exists any direction on the digitized surface along which periodic marks are concentrated. In this case, the *angular spectrum* can be used to determine the possible surface directionality.

From the *angular spectrum*, it can be extracted the angle corresponding to the highest accumulated radial amplitude value (A_{θ_max}). To check if the maximum value is dominant or not with respect to the other A_θ values, the SPIP program for surface analysis uses the *Surface texture direction index* ($Stdi$) which is expressed as [18]:

$$Stdi = \frac{\bar{A}_\theta}{A_{\theta\_max}} \tag{5}$$

where $\bar{A}_\theta$ is the average value of all accumulated radial amplitudes. If A_{θ_max} were similar to the rest of values, it would be close to the average value and therefore, the value of $Stdi$ would be near 1. In this case, there would be no directionality. On the contrary, if A_{θ_max} were far from the rest of values and much higher than the average value $\bar{A}_\theta$, the index $Stdi$ would be close to 0, showing a clear directionality.

5. Gaussian filtering of the point clouds digitized by the CH sensor

To remove the directionality effect observed in the point clouds obtained by the CH sensor, a Gaussian filter was applied by means of the function *imgaussfilt* of Matlab. Input points to this function should be equidistant along directions X and Y but the digitized points not always were regularly distanced so that it was necessary to generate

intermediate points by linear interpolation. This filter is controlled by means of a parameter σ, so that the greater the parameter, the greater the influence of the farthest points from the average as well as the smoother the surface obtained.

The laser spot of the CH sensor is asymmetric, so that its length along direction Y_{CH} is approximately 3 times the length w along X_{CH}. Therefore, instead of using a single parameter σ, two control parameters σ_X and σ_Y were used for filtering, where:

$$\sigma_X = 3 \cdot \sigma_Y \tag{6}$$

In order to take into account in the filtering process the normal distribution corresponding to the illumination of the points covered by the laser spot, σ_X and σ_Y were adjusted to the following values:

$$\sigma_X = 3k \cdot s \tag{7}$$

$$\sigma_Y = k \cdot s \tag{8}$$

where s is the standard deviation of the normal distribution, which can be calculated by Eq. (1), and k is a proportionality factor used to adjust the filter to different spot sizes.

5.1 Determination of factor k

In order to determine the values of k that provide the best filtering results, the evolution of index $Stdi$ for different values of this factor was represented in Fig. 8 corresponding to the two lenses used and the three positions within the DOF.

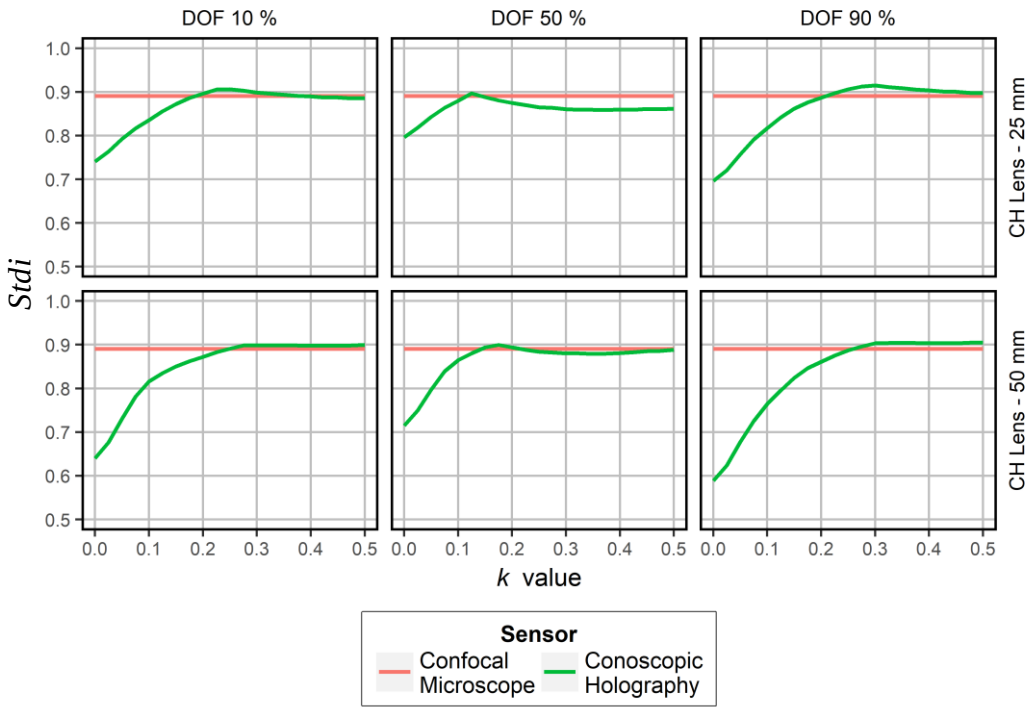

Fig. 8. Evolution of index $Stdi$ with respect to factor k

Before conducting the filtering process ($k = 0$) it was observed that the value of $Stdi$ for the CH sensor was very different to the case of the confocal microscope, which demonstrates the high directionality of the point clouds. As the value of k is increased in the filter, the value of $Stdi$ becomes closer for both sensors. In any case, care should be taken not to filter with very high values of k, since relevant information could be removed from the digitized surface.

As it can be seen in Fig. 8, a value of $k = 0.12$ will be sufficient for the surface located at 50% of the DOF (just at the *stand-off* distance) for both lenses. Value of $k = 0.2$ shall be required for the lens of 25 mm and the surface located at 10% and 90% of the DOF whereas a filter of $k = 0.25$ shall be necessary when using a lens of 50 mm for such locations in order to reach similar isotropy to the confocal microscope.

The need to apply a greater value of k for positions within the DOF farther from the *stand-off* distance could be explained since the spot size increases in such positions, showing higher directionality.

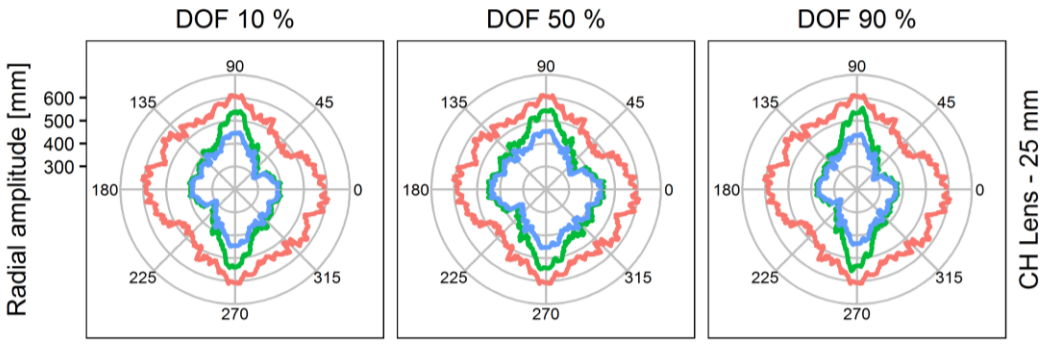

	Confocal	CH BF	CH AF	Confocal	CH BF	CH AF	Confocal	CH BF	CH AF
Stdi	0.89	0.74	0.89	0.89	0.74	0.89	0.89	0.70	0.89
k	-	-	0.20	-	-	0.12	-	-	0.20

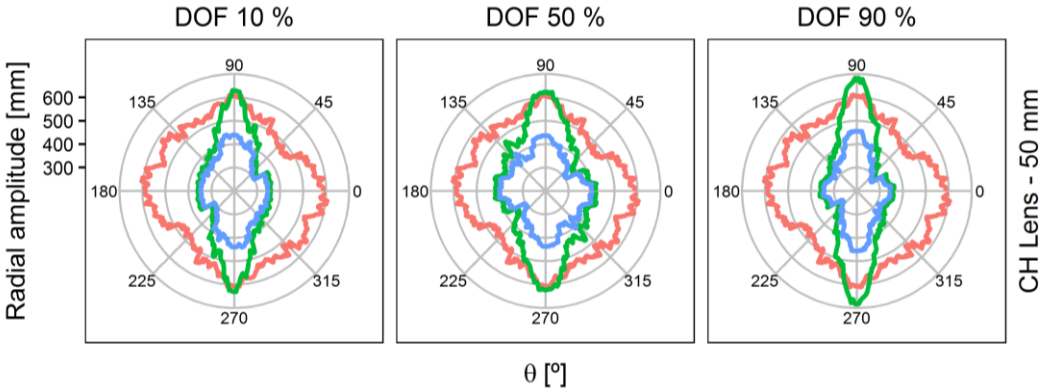

	Confocal	CH BF	CH AF	Confocal	CH BF	CH AF	Confocal	CH BF	CH AF
Stdi	0.89	0.64	0.89	0.89	0.71	0.90	0.89	0.59	0.90
k	-	-	0.30	-	-	0.12	-	-	0.30

BF: Before Filtering

AF: After Filtering

Confocal — CH BF — CH AF —

Fig. 9. Angular spectra of the EDM surface digitized by the confocal microscope and the CH sensor before and after filtering

5.2 Filtering results

Fig. 9 shows the angular spectra, before and after filtering, corresponding to the digitized EDM surface by means of the confocal microscope and the CH sensor when using lenses of 25 and 50 mm and for three locations within the DOF. As it can be seen, the microscope results show an *angular spectrum* with $Stdi = 0.89$, in accordance to the isotropy of EDM surface. On the contrary, the spectra obtained by the CH sensor before filtering, show high directionality with both lenses. This effect is visible in all positions within the DOF tested, being higher for the farthest positions from the *stand-off*. In particular, $Stdi = 0.59$ for the lens of 50 mm and the DOF position of 90%.

After applying the Gaussian filter, directionality shown in the *angular spectrum* of the digitized surface was reduced substantially and the spectrum presents a more uniform form, similar to that obtained with the confocal microscope. This way, the lens of 50 mm and the farthest position (90%) presents $Stdi = 0.90$, which is similar to that obtained by the confocal microscope.

Similarly, comparing the 2DFT graphs before and after filtering, it can be appreciated that directionality was eliminated for both lenses of 25 and 50 mm (Fig. 10).

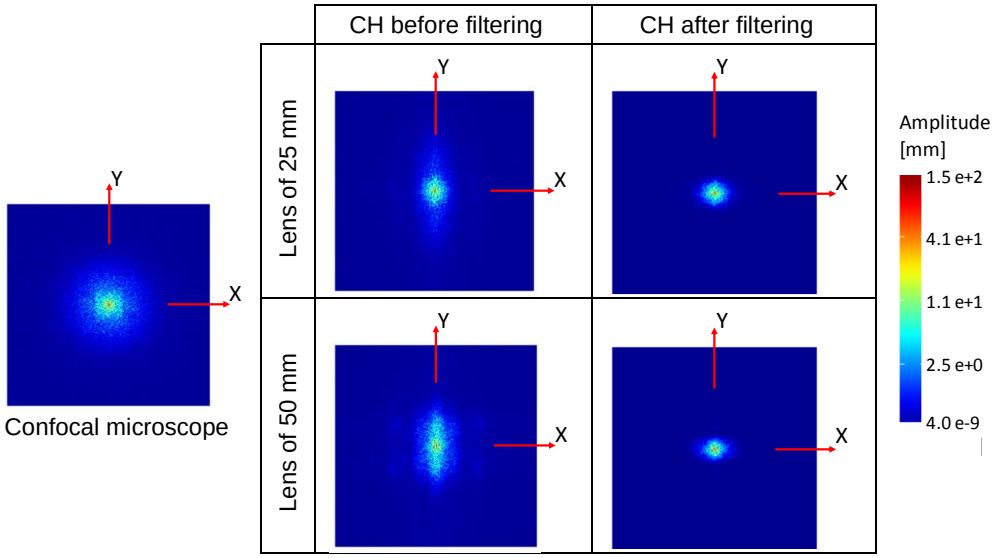

Fig. 10. 2DFT for the EDM surface digitized by the confocal microscope and the CH sensor.

The improvement achieved after the filtering process can also be realized comparing the point clouds before and after filtering. It can be seen in Fig. 11 that before filtering there is higher directionality of the point clouds obtained by the CH sensor (especially for the 50 mm lens) than the one by the confocal microscope. Nevertheless, directionality disappears after filtering so that all the point clouds become similar.

Confocal microscope CH sensor (25 mm) CH sensor (50 mm)

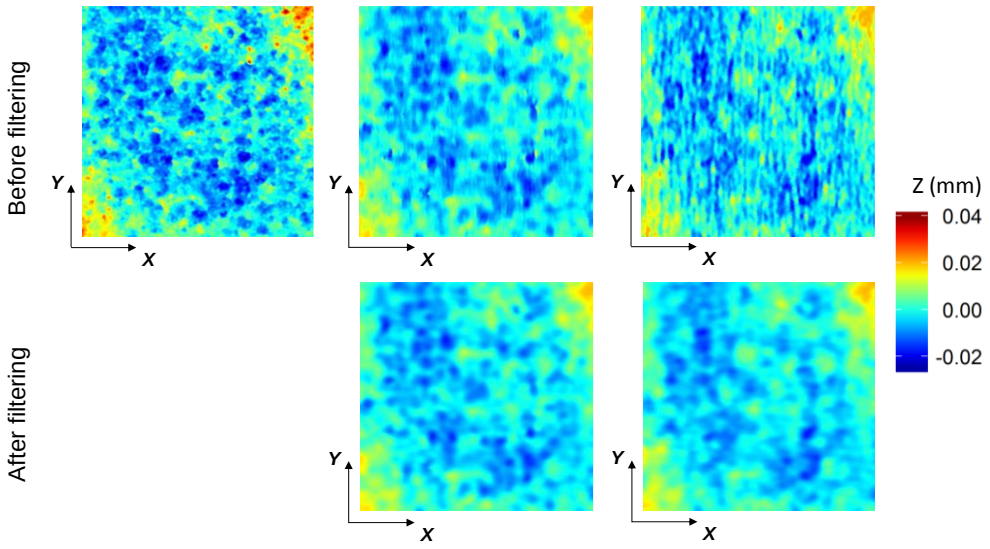

Fig. 11. Point clouds obtained by confocal microscope and CH sensor before and after filtering

6. Conclusions

This work shows that there exists a directional behaviour associated to the point clouds digitized by means of a CH sensor. This effect is mainly due to the size and shape of the laser spot and to the *lateral resolution* of measurement with the sensor. Moreover, due to the asymmetric shape of the laser spot, the effect of spot overlapping will be greater when performing the digitizing process along the largest direction of the spot instead of along the smallest one. Therefore, directionality increases.

To avoid any directional effect due to the surface, digitizing tests were performed on an EDM machined surface, which presents a uniform surface topography in all directions. Likewise, in order to favour the overlapping of laser spot and the appearance of directional effect, the digitizing was performed with a high density of points.

Using the representation of the 2D Fourier transform (2DFT), it was confirmed the existence of directionality in the point clouds obtained by the CH sensor, compared to the results by a confocal microscope, which were used as reference. It was also noticed that the directional effect came out along the largest spot direction and appeared repetitively under different working conditions (different lenses and locations within the DOF). Thus, this effect could be considered as a systematic error associated to the CH sensor and then, feasible to be eliminated. On the other hand, the use of the *angular spectrum* associated to the 2DFT transform made it possible to quantify the directionality by means of the index $Stdi$.

The application of a Gaussian filter was proposed to reduce the effect of directionality. Due to the asymmetry of the laser spot, two parameters (σ_X and σ_Y) were defined to control the filter, one associated to the largest laser spot direction and the other to the smallest one. Additionally, a factor of proportionality k was used to adjust the filter to different spot sizes.

The results achieved prove the effectiveness of the applied filter and the feasibility to define different factors k according to the *focal length* of the lens used and to the position of the digitized surface within the DOF of the CH sensor.

Acknowledgements

This work was supported by the Regional Ministry of Economy and Employment of the Principality of Asturias (Spain) (GRUPIN14-063) and the Government of the Principality of Asturias through the Programme "Severo Ochoa" 2014 of PhD grants for research and teaching (BP14-049).

References

[1] Chen F, Brown GM, Song M. Overview of three-dimensional shape measurement using optical methods. Optical Engineering 2000; 39(1):10–22.

[2] Blais F. Review of 20 years of range sensor development. Journal of Electronic Imaging 2004; 13(1):231–240.

[3] Sansoni G, Trebeschi M, Docchio F. State-of-the-art and applications of 3D imaging sensors in industry, cultural heritage, medicine and criminal investigation. Sensors 2009; 9:568–601.

[4] Sirat G, Psaltis D. Conoscopic Holography. Optics Letters 1985; 10(1):4–6.

[5] VDI/VDE 2617-6.2. Accuracy of coordinate measuring machines. Characteristics and their testing: Part 6.2. Guideline for the application of DIN EN ISO 10360 to coordinate measuring machines with optical distance sensors. 2005.

[6] Groot P de, Colonna de Lega X, Sykora D, Deck L. The meaning and measure of lateral resolution for surface profiling interferometers. OPN Optics & Photonics News 2012:10–13.

[7] Marshall GF, Stutz GE, editors. Handbook of Optical and Laser Scanning. 2nd ed. CRC Press, Taylor & Francis Group, 2012.

[8] Leach R, Giusca C, Henning A, Sherlock B, Coupland J. ISO Definition of Resolution for Surface Topography Measuring Instruments. Fringes 2013:405–410.

[9] ISO 16610-21. Geometrical product specifications (GPS). Filtration. Part 21: Linear profile filters. Gaussian filters. 2011.

[10] ISO 16610-61. Geometrical product specifications (GPS). Filtration. Part 61: Linear areal filters. Gaussian filters. 2015.

[11] Raja J, Muralikrishnan B, Fu S. Recent advances in separating of roughness, waviness and form. Precision Engineering 2002; 26:222–235.

[12] Dobrzanski P, Pawlus P. A study of filtering techniques for areal surface topography assessment. Proc. IMechE Part B: J. Engineering Manufacture 2011; 225(11):2097–2107.

[13] Li H, Cheung CF, Jiang XQ, Lee WB, To S. A novel robust Gaussian filtering method for the characterization of surface generation in ultra-precision machining. Precision Engineering 2006; 30:421–430.

[14] Dhanasekar B, Ramamoorthy B. Digital speckle interferometry for assessment of surface roughness. Optics and Lasers in Engineering 2008; 46(3):272–280.

[15] OEM Manual for Optimet's Mark10 (version 1). Optimet Manual P/N 3J06009 [Internet]. Optimet (Israel); [cited 2016 October 20]. Available from: http://www.optimet.com.

[16] Smith KB, Zheng YF. Point Laser Triangulation Probe Calibration for Coordinate Metrology. Journal of Manufacturing Science and Engineering 2000; 122(3):582–586.

[17] Stout KJ, Matthia T, Sullivan PJ, Dong WP, Mainsah E, Lou N, Zahouani H. Development of methods for the characterization of roughness in three dimensions. EC Brussels, DGXII, BCR programme, Report EUR 15178 EN, ISBN 0 7044 1313 2, 1993.

[18] Reference manual of the SPIP.

http://www.spip.imagement.com/WebHelp6/Default.htm